Chemical Research in Toxicology

pubs.acs.org/crt

Article

Vegetable Activated Charcoal for Human Consumption Reduces Selected PFAS Levels in a Bile Secretion Model: Cues on Its Possible Clinical Use

Alessandro Bonetto [§] Luca De Toni [§] Andrea Di Nisio Laura Pagnin Alberto Ferlin Antonio Marcomini * and Carlo Foresta

Cite This: *Chem Res Toxicol* 2026 39 900−907

Read Online

ACCESS | Metrics & More | Article Recommendations | Supporting Information

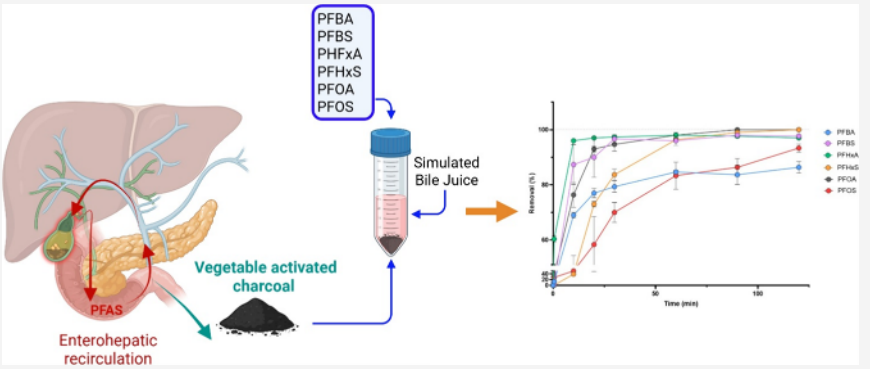

ABSTRACT: Perfluoroalkyl substances (PFAS) are pollutants with relevant accumulation in humans, and the enterohepatic circulation of PFAS secreted in bile sustains their persistence. A significant increase in fecal excretion has been experimentally assessed with the use of oral adsorbents with negligible gut absorption. Here, we evaluated *in vitro* the use of activated charcoal (AC) for human consumption, as sorption material for a panel of PFAS, such as, perfluoro-butanoic acid (PFBA), perfluoro-butanesulfonic acid (PFBS), perfluoro-hexanoic acid (PFHxA), perfluoro-hexanesulfonic acid (PFHxS), perfluoro-octanoic acid (PFOA), and perfluoro-octanesulfonic acid (PFOS), in an experimental simulated bile juice (SBJ). The aim was to obtain preliminary data for possible clinical applications to reduce PFAS blood levels in humans. PFAS concentrations in experimental samples were quantified by liquid chromatography−mass spectrometry. In kinetic tests, equimolar solutions of single PFAS in SBJ were incubated with AC at 37 °C up to 120 min, and the time-dependent reduction of PFAS concentration was monitored. In thermodynamic tests, PFAS solutions in SBJ were incubated at increasing concentrations with AC for 24 h at 37 °C and the concentrations at equilibrium evaluated. Results were finally fitted with available models in order to characterize the PFAS interaction with AC. All PFAS showed more than 80 sorption on activated charcoal from simulated bile juice within 120 min. This suggests rapid and nearly complete removal. Modeling analysis indicated that the pseudo-first-order kinetic model best described short-chain PFAS, while PFOS and PFOA fitted better with the Elovich model. Thermodynamic analysis showed a general fitting with the Freundlich model, presumptive of a heterogeneous binding model. PFOS binding was concentration-dependent and was better described by the Sips model. These data are suggestive of a potential noninvasive intervention strategy to increase fecal PFAS excretion through the dietary use of AC, in order to mitigate health issues associated with PFAS exposure.

INTRODUCTION

Perfluoroalkyl substances (PFAS) are anthropogenic chemicals with a partially (poly) or fully (per) fluorinated alkyl chain. Food and drinking water are primary sources of human exposure, though other environmental routes (e.g., inhalation) can contribute. Serum PFAS levels, recognized as exposure markers, are typically higher in males than females.[1−4] The estimated plasma half-lives of two long-chain legacy compounds, perfluoro-octanesulfonic acid (PFOS) and perfluoro-octanoic acid (PFOA), are 5.4 and 2.3−3.8 years, respectively.[4] Although much of the PFAS burden is protein-bound in plasma, relevant accumulation occurs in bile, skeletal muscle, liver, and kidneys.[1,5] Tissue accumulation is thought to be sustained by enterohepatic circulation (EHC), being actively secreted in bile

Received: November 27, 2025
Revised: April 7, 2026
Accepted: April 14, 2026
Published: May 5, 2026

and subsequently reabsorbed in the gut with minimal fecal elimination.[6,7]

No therapeutic protocols are currently approved to reduce PFAS blood levels in humans. Experimental strategies have included long-term phlebotomy and apheresis.[8,9] Alternative approaches have taken advantage of EHC to promote PFAS removal using oral adsorbents with negligible gut absorption. In murine models, the bile acid sequestrant cholestyramine enhanced fecal excretion of PFAS.[10] Case reports in humans confirmed that cholestyramine (4 g three times daily for 28 weeks) significantly reduced circulating PFOS, PFOA, and PFHxS.[9,11] However, the standard 12 g/day dosage is poorly tolerated, with high rates of constipation and therapy discontinuation.[12] The use of colesevelam, a more recent and better tolerated bile acid sequestrant, showed a clear secretory effect on PFHxS and PFOS but a weak and less consistent impact on PFOA.[10]

Activated charcoal is a recognized treatment for PFAS removal from drinking water.[13−16] In human adults, the oral use of vegetable activated charcoal (AC) is approved for acute drug intoxication, at a typical dose of 30−50 g as a gastric bolus. AC is also indicated in subchronic conditions, such as bloating and uremic pruritus, at an overall daily dose of 6 g for up to 6 weeks.[17,18] Taken together, this evidence suggests the potential of oral AC to reduce elevated PFAS levels in highly exposed individuals, possibly in combination with a choleretic substance in order to stimulate bile secretion. In this study, we evaluated the possible use of AC approved for human consumption as sorption material for selected long-chain and short-chain PFAS in an experimental bile secretion model, providing preliminary cues on its possible clinical application.

EXPERIMENTAL PROCEDURES

Chemicals

Vegetable activated charcoal for use in food (cat 0189−1000-g), produced by coconut combustion and activated with water steam, was purchased from Galeno (Carmignano, Prato, Italy). The reported technical data of AC were as follows: average grain size of 15−35 μm, with 90 less than 74 μm, iodine number of approximately 1000 mg/g, and average surface area of 1800 m^2/g. Perfluoro-butanoic acid (PFBA, 98 , cat. no. 164194−25G), perfluoro-butanesulfonic acid (PFBS, 97 , cat. no. 562629−25G), perfluoro-hexanoic acid (PFHxA, 97 , cat 29226−5 ML), potassium perfluoro-hexanesulfonate (PFHxK, cat. no. 88818−10MG), heptadecafluoro-octanesulfonic acid potassium salt (PFOK, cat. no. 95181−25MG), and PFOA (95 , cat. no. 17148−25g) were purchased from Merck-Sigma (Milano, Italy). Mass-labeled PFAS Mixture/Solution (cat MPFAC-24ES) was purcahed from Wellington Laboratories (Southgate, Ontario, Canada). Simulated Bile Juice (SBJ, BZ263, Biochemazone, Alberta, Canada) was used as a bile secretion model, given the specific qualitative composition including both organic and inorganic ingredients, as per the certificate of analysis.

Experimental Conditions

Experimental conditions were defined according to an estimated overall daily oral dose of AC of 7 g/day, fractionated into two single doses of 3.5 g each, to be taken away from meals. Considering a daily production of bile secretion of approximately 600 mL/day divided into four fractions, each of 150 mL, the resulting carbon/bile secretion ratio was 23.3 mg/mL. For operational simplicity, in order to reduce weighing errors due to the low handling of the material, a solid/liquid ratio of 30 mg/mL was considered.

Using a reference test concentration of PFOA of 100 ng/mL, the same molar test concentration was used for each individual selected PFAS (Table S1). Operationally, each PFAS was weighed into a 50 mL polypropylene (PP) test tube, dissolved with 50 mL of a 9:1 ultrapure water:methanol (UPW:MeOH) solution and named Stock1 solution. The Stock1 solutions of each PFAS were then appropriately diluted with SBJ, obtaining 50 mL of an intermediate Working1 solution at an individual concentration of 604 nmol/L.

Test samples were obtained by weighing 750 mg of activated carbon in a 50 mL PP tube to which 15 mL of SBJ was added and let to equilibrate for 12 h at 37 °C under orbital shaking at 250 rotations per minute (rpm).

In kinetic tests, 10 mL of Working1 solutions of each PFAS were added into equilibrated AC/SBJ suspension, obtaining the same test concentration of 241 nmol/L, compatible with the highest mean plasma levels reported long-chain PFAS.[1,10] Each sample was homogenized by vortexing for 5 s and then let to incubate at 37 °C under orbital shaking at 250 rpm up to 120 min. Each PFAS was tested in triplicate. Control sample (CTRL), in which AC was omitted, was tested in singleton based on the precision and consistency of the method. Test samples underwent consecutive withdrawals of 250 μL aliquots immediately after adding Working1 solutions and after 0.5, 10, 20, 30, 60, 90, and 120 min. Aliquots were immediately collected, filtered with 0.45 μm regenerated cellulose filters (Claristep, Sartorius, Gottinga, Germany), and collected into 0.3 μL PP vials. After filtration, 5 μL of each aliquot was diluted 100-fold with the diluent solution to a final volume of 500 μL. 10 μL portions of internal standards (IS) were then added to each diluted aliquot and stored at 4 °C until analysis.

In thermodynamic tests, 300 mg of AC was dispersed in 10 mL of SBJ in a 15 mL polypropylene (PP) test tube, and appropriate amounts of the Working1 solutions were added. Samples were maintained for 24 h at 37 °C under constant shaking at 250 rpm by an orbital shaker. Finally, samples were centrifuged at 11,139g (Eppendorf Centrifuge 5910 Ri) and 5 μL of supernatant was diluted 100-fold with the diluent solution to a final volume of 500 μL in 0.7 mL poly propylene vials. 10 μL of internal standard was then added to the diluted samples and then stored at 4 °C until quantitative analysis.

Liquid Chromatography−Mass Spectrometry

Quantitative analysis was performed with a liquid chromatograph coupled to a mass detector (LC-MS/MS TQ Absolute, Waters). The chromatographic separation was performed using a 1.7 μm, 2.1 × 50 mm BEH C18 column, and the mobile phases were 2 mM NH4Ac in UPW and 2 mM in NH4Ac MeOH:AcCN 1:1 mixuture. The method involved the quantification of PFAS through correction with a labeled IS and using a 7-point calibration curve (Table S2). Vials were maintained at 10 °C for the entire duration of the analysis, using 50 μL for each run. Table S3 shows the mass spectrometer conditions. The analysis was conducted in negative mode, with a source temperature of 100 °C, desolvation temperature of 350 °C, desolvation flow rate of 900 L/h, and gas cone of 150 L/h. Method validation, by replicate analyses on spiked samples across multiple concentration levels, showed a relative standard deviation (RSD) ranged between 2 and 8 , demonstrating precision and consistency.

Modeling Analysis

In kinetic studies, in order to characterize the nature of interactions between PFAS and AC in bile simulants and to address the possible influence of PFAS chain length on the adsorption rate, data were fitted with pseudo-first-order (Lagergren), pseudo-second-order (Ho), and Elovich kinetic models. Applied models were as follows:

Lagergren or Pseudo-First Order pFO).

$$\ln q - q_t) \quad \ln q - k_1 t$$

where: q_e is the molar concentration adsorbed at equilibrium; q_t is the molar concentration adsorbed at time t; and k_1 is the kinetic constant.

Ho Equation or Pseudo-Second Order pSO).

$$\frac{t}{q_t} = \frac{1}{k_2 q^2)} \quad \frac{t}{q}$$

where q_e is the molar concentration adsorbed at equilibrium; q_t is the molar concentration adsorbed at time t; and k_2 is the kinetic constant.

Elovich Equation.

https://doi.org/10.1021/acs.chemrestox.5c00510
Chem Res Toxicol 2026 39 900−907

Table 1. Quantification of the Selected Perfluoroalkyl Substances PFAS) in Kinetic Tests of Sorption on Vegetable Activated Charcoal AC) for Human Consumption[b]

	PFAS (ng/mL)					
time (min)	PFBA	PFBS	PFHxA	PFHxS	PFOA	PFOS
CTRL	55.4 ± 0.4	96.2 ± 1.5	75.1 ± 0.3	139.2 ± 1.8	113.2 ± 3.1	150.0 ± 5.4
0.5	50.9 ± 1.3[a]	96.6 ± 6.9	29.9 ± 0.5[a]	143.0 ± 6.0	69.1 ± 6.2[a]	109.0 ± 16.1[a]
10	20.0 ± 0.5[a]	12.4 ± 7.2[a]	2.9 ± 0.1[a]	85.7 ± 2.5[a]	27.2 ± 4.7[a]	75.3 ± 6.4[a]
20	15.4 ± 0.9[a]	9.8 ± 7.3[a]	2.2 ± 0.2[a]	38.2 ± 1.0[a]	8.5 ± 0.9[a]	62.5 ± 15.5[a]
30	14.2 ± 1.3[a]	3.2 ± 1.3[a]	2.0 ± 0.1[a]	23.4 ± 2.6[a]	6.7 ± 2.8[a]	45.1 ± 5.3[a]
60	11.2 ± 0.3[a]	3.9 ± 1.9[a]	1.8 ± 0.0[a]	5.6 ± 0.6[a]	3.0 ± 0.7[a]	25.1 ± 6.9[a]
90	11.9 ± 2.1[a]	1.9 ± 0.1[a]	1.9 ± 0.4[a]	2.3 ± 0.2[a]	0.9 ± 0.02[a]	20.3 ± 5.0[a]
120	10.3 ± 1.0[a]	2.1 ± 0.4[a]	2.3 ± 0.2[a]	0.8 ± 0.2[a]	0.2 ± 0.03[a]	9.8 ± 1.8[a]
CTRL-AC	2.81 ± 1.1	<0.1	<0.1	0.46 ± 0.3	0.46 ± 0.4	<0.1

[a]Significance: $P < 0.0001$ vs respective CTRL. [b]Abbreviations: PFBA, perfluoro-butanoic acid; PFBS, perfluoro-butanesulfonic acid; PHFxA perfluoro-hexanoic acid; PFHxS, perfluoro-hexanesulfonic acid; PFOA, perfluoro-octanoic acid; PFOS, perfluoro-octanesulfonic acid; CTRL, control sample in which AC was omitted, CTRL-AC, control sample of AC in which PFASs were omitted. All standard deviations refer to three independent experiments. Standard deviations of CTRL and CTRL-AC result from three consecutive assessments of the same sample.

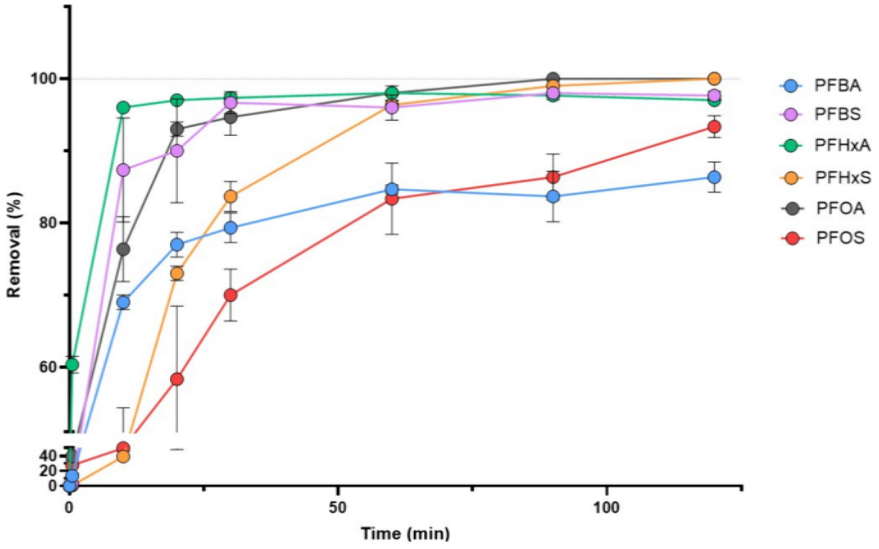

Figure 1. Experimental evaluation of the time-dependent removal of a panel of perfluoroalkyl substances from a simulated bile juice by activated charcoal for human consumption. Data are reported as the mean value ± standard deviation of a technical replicate. Abbreviations: PFBA, perfluoro-butanoic acid; PFBS, perfluoro-butanesulfonic acid; PHFxA perfluoro-hexanoic acid; PFHxS, perfluoro-hexanesulfonic acid; PFOA, perfluoro-octanoic acid; PFOS, perfluoro-octanesulfonic acid.

$$_t = \frac{1}{\beta}\ln\ 1 \quad \alpha\beta t)$$

where q_t is the molar concentration adsorbed at time t; is the initial absorpion rate; and β is the parameter is related to the heterogeneity of the adsorption sites.

In thermodynamic studies, in order to evaluate the role of sorbent saturation and to address the mechanism of adsorption mechanism (e.g., chemo-adsorption *vs* physi-adsorption), a fitting analysis with classical thermodynamic models, namely, the Langmuir isotherm, Freundlich isotherm, Temkin isotherm, and Sips model, was performed. The reference models were as follows:

Langmuir Isotherm.

$$q_e = \frac{q_{\max} K_L\ _e}{K_L\ _e}$$

where q_e is the molar concentration adsorbed at equilibrium (mol/g); C_e is the molar concentration at equilibrium (mol/L); $q_{\max}$ is the maximum adsorption capacity (mol/g); and K_L is the Langmuir constant.

Freundlich Isotherm.

$$q_e \quad K_F\ _e^{\ 1\ n}$$

where q_e is the molar concentration adsorbed at equilibrium (mol/g); C_e is the molar concentration at equilibrium (mol/L); n is the surface heterogeneity; and K_F is the Freundlich constant.

Temkin Isotherm.

$$q_e \quad \frac{RT}{b_T}\ln \quad _T C_e)$$

where q_e is the molar concentration adsorbed at equilibrium (mol/g); C_e is the molar concentration at equilibrium (mol/L); b_T is the adsorption energy (J/mol); A_T is the Temkin constant; R is the universal gas constant (J/mol × K); and T is the absolute temperature (K).

Sips Model.

$$q_e = \frac{q_{\max}\ K_S\ _e)^n}{1 \quad K_S\ _e)^n}$$

where q_e is the molar concentration adsorbed at equilibrium (mol/g); C_e is the molar concentration at equilibrium (mol/L); $q_{\max}$ is the

https://doi.org/10.1021/acs.chemrestox.5c00510
Chem Res Toxicol 2026 39 900−907

Table 2. Analysis of Kinetic Model Fitness for Perfluoroalkyl Substance PFAS) Absorption to Vegetable Activated Charcoal for Human Use AC), According to Pseudo-First-Order pFO), Pseudo-Second-Order pSO), or Elovich Models[a]

PFAS	replicate	model	R^2	RMSE	q_e	k_1	k_2		β
PFBA	1	pFO	0.9866	3.05×10^{-04}	0.0067	0.172			
		pSO	**0.9976**	**1.29 10^{-04}**	**0.0071**		**44.2**		
		Elovich	0.9667	4.82×10^{-04}				0.007954	890
	2	pFO	0.9952	1.93×10^{-04}	0.0069	0.153			
		pSO	**0.9973**	**1.45 10^{-04}**	**0.0074**		**36.1**		
		Elovich	0.9550	5.88×10^{-04}				0.006151	824
	3	pFO	0.9972	1.41×10^{-04}	0.0067	0.166			
		pSO	**0.9935**	**2.16 10^{-04}**	**0.0071**		**45.0**		
		Elovich	0.9376	6.68×10^{-04}				0.007634	892
PFBS	1	**pFO**	**0.9953**	**2.99 10^{-04}**	**0.0104**	**0.236**			
		PSO	0.9781	6.45×10^{-04}	0.0111		34.4		
		Elovich	0.8954	1.41×10^{-03}				0.012745	568
	2	**pFO**	**0.9924**	**3.76 10^{-04}**	**0.0103**	**0.233**			
		pSO	0.9762	6.68×10^{-04}	0.0110		33.7		
		Elovich	0.8963	1.39×10^{-03}				0.011909	567
	3	**pFO**	**0.9752**	**7.11 10^{-04}**	**0.0104**	**0.135**			
		pSO	0.9669	8.21×10^{-04}	0.0113		18.5		
		Elovich	0.9117	1.34×10^{-03}				0.005265	486
PFHxA	1	**pFO**	**0.9998**	**3.86 10^{-05}**	**0.0077**	**1.956**			
		pSO	0.9998	3.89×10^{-05}	0.0078		413.9		
		Elovich	0.9739	4.21×10^{-04}				25.43843	1889
	2	**pFO**	**0.9998**	**3.95 10^{-05}**	**0.0077**	**1.948**			
		pSO	0.9998	4.09×10^{-05}	0.0078		411.4		
		Elovich	0.9735	4.24×10^{-04}				24.3875	1883
	3	**pFO**	**0.9999**	**2.56 10^{-05}**	**0.0077**	**1.893**			
		pSO	0.9995	5.70×10^{-05}	0.0078		394.5		
		Elovich	0.9702	4.50×10^{-04}				18.86691	1849
PFHxS	1	**pFO**	**0.9974**	**2.36 10^{-04}**	**0.0115**	**0.058**			
		pSO	0.9904	4.49×10^{-04}	0.0134		5.2		
		Elovich	0.9739	7.42×10^{-04}				0.001854	352
	2	**pFO**	**0.9931**	**3.87 10^{-04}**	**0.0116**	**0.058**			
		pSO	0.9817	6.28×10^{-04}	0.0135		5.1		
		Elovich	0.9616	9.11×10^{-04}				0.001787	345
	3	**pFO**	**0.9954**	**3.10 10^{-04}**	**0.0116**	**0.058**			
		pSO	0.9864	5.36×10^{-04}	0.0135		5.1		
		Elovich	0.9684	8.15×10^{-04}				0.00186	351
PFOA	1	pFO	0.9770	4.86×10^{-04}	0.0083	1.348			
		pSO	0.9861	3.78×10^{-04}	0.0085		201		
		Elovich	**0.9950**	**2.27 10^{-04}**				**0.1053**	**945**
	2	pFO	0.9131	1.00×10^{-03}	0.0089	0.155			
		pSO	0.9685	6.03×10^{-04}	0.0087		94.9		
		Elovich	**0.9845**	**4.23 10^{-04}**				**0.0395**	**877**
	3	pFO	0.9564	5.71×10^{-04}	0.0087	1.044			
		pSO	0.9776	4.09×10^{-04}	0.0089		121		
		Elovich	**0.9794**	**3.92 10^{-04}**				**0.1009**	**984**
PFOS	1	pFO	0.9561	6.69×10^{-04}	0.0089	0.053			
		pSO	0.9705	5.48×10^{-04}	0.0102		6.73		
		Elovich	**0.9843**	**4.00 10^{-04}**				**0.002**	**534**
	2	pFO	0.8649	1.12×10^{-03}	0.0088	0.067			
		pSO	0.8910	1.01×10^{-03}	0.0097		11.2		
		Elovich	**0.9546**	**6.48 10^{-04}**				**0.012**	**785**
	3	pFO	0.7904	1.31×10^{-03}	0.0085	0.082			
		pSO	0.8271	1.19×10^{-03}	0.0091		16.5		
		Elovich	**0.9525**	**6.25 10^{-04}**				**0.037**	**968**

[a]Abbreviations: PFBA, perfluoro-butanoic acid; PFBS, perfluoro-butanesulfonic acid; PHFxA perfluoro-hexanoic acid; PFHxS, perfluoro-hexanesulfonic acid; PFOA, perfluoro-octanoic acid; PFOS, perfluoro-octanesulfonic acid; R^2, determination coefficient; RMSE, root-mean-square error; q_e, molar concentration adsorbed at equilibrium; k_1, pFO kinetic constant; k_2, pSO kinetic constant; , initial absorpion rate; β, parameter related to the heterogeneity of the adsorption sites; Parameters of the best describing model for each replicate, according to the highest R^2 value and lowest RMSE value, are in bold.

https://doi.org/10.1021/acs.chemrestox.5c00510
Chem Res Toxicol 2026 39 900−907

Table 3. Analysis of Thermodynamic Model Fitness for Perfluoroalkyl Substance PFAS) Absorption to Vegetable Activated Charcoal for Human Use AC), According to the Langmuir Isotherm, Freundlich Isotherm, Temkin Isotherm, or Sips Model[a]

PFAS	model	^{2}	RMSE	q_{max}	K_L	K_F	n	A_T	b_T	K_S
PFBA	Langmuir	0.974	0.005	44714	0.000					
	Freundlich	**0.984**	**0.004**			**2.187**	**0.871**			
	Temkin	0.951	0.008					74.9	42367	
	Sips	0.984	0.004	0.495			1.32			8.77
PFBS	Langmuir	0.903	0.007	0.114	345					
	Freundlich	**0.948**	**0.005**			**0.268**	**3.787**			
	Temkin	0.941	0.006					5591	120617	
	Sips	0.948	0.005	1626			0.26			0.000
PFHxA	Langmuir	0.824	0.012	27770	0.000					
	Freundlich	**0.966**	**0.005**			**34.00**	**0.474**			
	Temkin	0.627	0.018					121	66348	
	Sips	0.966	0.005	4102			2.11			0.008
PFHxS	Langmuir	0.818	0.005	0.057	101					
	Freundlich	**0.936**	**0.003**			**0.159**	**2.670**			
	Temkin	0.726	0.007					38098	453693	
	Sips	0.936	0.003	5843			0.37			0.000
PFOA	Langmuir	0.953	0.006	0.112	79					
	Freundlich	0.872	0.010			0.323	2.37			
	Temkin	0.850	0.010					1934	141784	
	Sips	**0.962**	**0.005**	**0.098**			**1.37**			**571**
PFOS	Langmuir	0.955	0.003	0.088	141					
	Freundlich	0.844	0.006			0.191	3.44			
	Temkin	0.907	0.004					1601	135889	
	Sips	**0.976**	**0.002**	**0.079**			**1.47**			**1781**

[a]Abbreviations: PFBA, perfluoro-butanoic acid; PFBS, perfluoro-butanesulfonic acid; PHFxA perfluoro-hexanoic acid; PFHxS, perfluoro-hexanesulfonic acid; PFOA, perfluoro-octanoic acid; PFOS, perfluoro-octanesulfonic acid; R^2, determination coefficient; RMSE, root-mean-square error; q_{max}, molar concentration adsorbed at equilibrium; K_L, Langmuir constant; K_F, Freundlich constant; n, surface heterogeneity; A_T, Temkin constant; b_T, adsorption energy; K_S, Sips constants. Parameters of the best describing model, according to the highest value of R^2 and the lowest value of RMSE for each replicate, are in bold.

maximum adsorption capacity (mol/g); n is the surface heterogeneity; and K_S is the Sips constants.

Statistical Analysis

Statistical analysis was performed with GraphPad Prism 10.6.1 (GraphPad Software, Boston, Massachusetts USA). One-way analysis of variance (ANOVA) followed by Tukey's post hoc test for multiple comparisons among time points was performed to assess the effect of contact time on the sorption kinetics of the selected PFAS.

RESULTS AND DISCUSSION

Kinetic Tests

Preliminary experiments were performed throughout an overall observation time of 48 h, showing the achievement of a steady state adsorption rate of PFAS on AC within 120 min (Figure S1). Subsequent experiments then focused on this observation period, with more frequent sampling times in the first 60 min.

Results of PFAS quantification, distinguished by analyte and sampling time, are reported in Table 1. Importantly, PFAS content in naive AC (CTRL-AC) was found at concentrations below the limit of detection (0.1 μg/L), with the exception of PFBA, PFHSX, and PFOA for which background values were, respectively, 2.81, 0.46, and 0.46 0.1 μg/L. This was likely attributable to the ubiquity of PFAS, appearing to be present in detectable concentrations in any matrix (e.g., surface water, drinking water). However, these background values represented less than 0.5 of the control values, allowing for the evaluation of 99.5 removals.

In general, a discrepancy was observed between the concentration of individual PFAS at time t = 0 and that of the control sample in which AC was omitted. This suggests that, especially for highly hydrophobic carboxylic PFAS, such as the long-chain PFOA, despite sampling operations performed within 30 s from AC addition, the adsorption rate on AC was very high, resulting in a significant reduction of PFAS concentration. This evidence was observed for all of the long-chain PFAS evaluated. This is consistent with the octanol−water partition coefficients (log K_{ow}) for the analyzed PFAS, which represents a good descriptor of PFAS partitioning in aqueous solution (Table S4). In general, it was observed that the higher this parameter, the greater was the reduction of PFAS concentration over the first 30 s of exposure to AC.

The percentage-removal profile for each individual PFAS by the AC, corrected for background values, is reported in Figure 1. Within 120 min, the removal profiles of PFBS, PFHxA, PFHxS, and PFOA were compatible with the achievement of a steady state condition, with stable removal percentages of ∼100 . A relevant deviation from this pattern was observed for PFOS, whose sorption kinetic appeared slower, achieving 83.3 after 1 h, compared to >95 for the aforementioned PFAS, despite the achievement of a final removal of >90 at 120 min. Differently, PFBA achieved a final removal rate of 86 at the end of the experiment.

The data were fitted with pseudo-first-order (Lagergren), pseudo-second-order (Ho), and Elovich kinetic models in order to provide a kinetic model of interactions between PFAS and AC in bile secretion and to address the role of the carbon chain length on the initial adsorption rate. Results of kinetic parameter modeling are reported in Table 2. Within the limits of

https://doi.org/10.1021/acs.chemrestox.5c00510
Chem Res Toxicol 2026 39 900−907

experimental variability, the adsorption of PFAS by AC in an aqueous environment were better described by a pSO model, especially for long-chain PFAS that better adapts to adsorption mechanisms involving chemical bonds or electron exchange, thus not only relying on physical surface forces. This model is characterized by a rapid initial adsorption rate due to the large excess of free sites followed by a gradual approach to equilibrium. In particular, different from the other tested PFASs with shorter carbon chain, the Elovich model better described the kinetic profile of PFOA and PFOS.

Thermodynamic Tests

Raw data of concentration at equilibrium (C_e) *vs* initial concentration (C_0) curves for each tested PFAS are reported in Figure S2. In qualitative terms, long-chain PFAS, namely, PFOA and PFOS, showed a nearly linear increase of C_e for low C_0 values followed by a nearly exponential surge. On the other hand, short-chain PFAS showed a nearly linear increase of C_e throughout the whole range of C_0.

Results of fitting analysis on thermodynamic models are reported in Table 3 and corresponding graphical representations are reported in Supporting Information, Figure S3. Several models have been adopted, whose detailed description has been recently reviewed by Mozaffari Majd et al.[19] Briefly, the Langmuir isotherm in its linear form relies on the homogeneous surface of the adsorbent material, with energetically equivalent sites forming a single layer of sorped molecules with negligible mutual interaction. The Freundlich model, on the other hand, assumes that the material surface is heterogeneous, with the sorption energy varying according to the active sites and the possible formation of a multilayer of adsorbed molecules. The Temkin equation is widely used to study the thermodynamic behavior, as it links the adsorption energy to the surface coverage. However, this relationship is less reliable when saturation occurs at high concentrations. Finally, the Sips equation describes intermediate situations, describing Langmuir-type behavior at high concentrations and Freundlich-type behavior at low concentrations and considering the heterogeneity of the active sites. The sorption of short-chain C4 PFAS (PFBA, PFBS) is best described by the Freundlich model, showing a nearly linear dependence of the adsorbed amount on the residual concentration (C_e) associated with low levels of saturation of active sites or low binding energy. This evidence is consistent with the chemical−physical characteristics of short-chain PFAS, which, compared to their long-chain counterparts, have lower octanol−water partition coefficients (Table S3). The highest values of K_L have been observed for long-chain PFAS, confirming that the chain length is an important parameter in the adsorption of PFAS in carbon matrices such as activated carbon. However, chain length might affect the steric hindrance of the molecules, hampering the diffusion and adsorption into very narrow pores, thus also limiting their maximum adsorption capacity. This hypothesis is confirmed by the calculated q_{max} value of PFAS and PFOA, by the SIPS model, which is lower than that of PFBA.

To the best of our knowledge, this is the first study providing evidence for a significant sorption of legacy PFAS of activated charcoal from a human bile secretion model. Considering the complex composition of bile, including bile acids, electrolytes, and organic metabolites that can compete for the absorption to AC, the observed net removal of at least 80 of the compounds sustains the possible tole of AC to reduce the pool of PFAS susceptible to enterohepatic recirculation, thus promoting their fecal elimination.[10]

At first, the kinetic and thermodynamic adsorption of a PFAS panel on a commercially available AC for oral use were characterized from a bile secretion model. Importantly, the experimental conditions were adjusted to match the approved daily oral dose of AC for the reduction of excessive intestinal gas accumulation and bloating.[20] Our results show that incubating with AC is linked to an average decrease in PFAS levels by more than 80 through adsorption, which generally reaches equilibrium within 2 h. For medium- to short-chain PFAS, the adsorption follows the Freundlich model, indicated by a heterogeneous binding mode based on the surface sorption energy, availability of active sites, and possible multilayer formation. Differently, long-chain PFAS are better described by the Sips model, relying on a homogeneous or heterogeneous binding mode according to the concentation of the sorped compound.[19] These findings are consistent with recent work by Abulikemu et al., who found that perfluoroalkyl carboxylic acids fit well with the Freundlich model, whereas PFOS deviated from this pattern depending on the granulometry of the adsorbent material.[21] Interestingly, previous data from Abulikemu showed the achievement the sorption equilibrium between 6 and 18 h for PFHxS, different from the 2 h observed in the current study.[21] This discrepancy might be due to the execution of all experiments at 37 °C, which is largely compatible with a rate-doubling compared to room temperature.

Of note, the maximum adsorption capacities of AC measured in the present study are approximately 100 times lower compared to those reported for other aqueous matrices.[22] This difference can be attributed not only to the limitations of the test, since real conditions were simulated without bringing the material to saturation, but more importantly to the different composition of natural aqueous matrices compared to the BJC.[23] In fact, compared to the 0.05−0.2 solute content of natural mineral waters, essentially constituted of inorganic salts, bile secretion typically shows a 5 content of organic solutes including 61 bile acids surfactants, 12 fatty acids, and 9 cholesterol.[23,24] Accordingly, it can be speculated that, given the amphiphilic nature of the abovementioned organic compounds, competition/interference processes may have been established with PFAS at the surface binding to the AC, thus generating possible deviations from the models typically considered as reliable.[25] To this regard, sorption kinetics for PFOA and PFOS on AC are better described by the Elovich model, different from the other tested PFAS. Data from Militao et al., using rice straw-derived biochar, showed a pSO-like fitting for PFOS adsorption in purified water.[26] Differently, the Elovich model was the best fitting model of lead ion adsorption on coconut AC as described by Largitte and Pasquier.[27] It can thus be essentially speculated the possible modification of the hydrophilic−lipophilic balance of long-chain PFAS by bile salts, being more hydrophobic and susceptible to the surfactant activity of the latter, resulting in the first binding to the lower energy surface sites of the carbon saturate followed by the shifts to the higher energy surface sites, resulting in a decrease of the sorption rate.[27] Nonetheless, our results suggest that the use of vegetable carbon associates with an average adsorption efficiency greater than 80 for all PFAS, even at the mg/L range reported for bile secretion.[5−7] As a limitation, we acknowledge that the potential modification of AC sorbent activity by the exposure to the sequential gastric and duodenal fluid environment remains to be addressed. In addition, given the rather nonspecific adsorbent activity of

https://doi.org/10.1021/acs.chemrestox.5c00510
Chem Res Toxicol 2026 39 900−907

AC, careful consideration of appropriate dosing is necessary to minimize possible nutrient malabsorption.[28]

Our preliminary findings indicate the possibility of a noninvasive pharmacological intervention to enhance fecal excretion of PFAS, particularly following the reduction or cessation of exposure to these substances. Accordingly, the dietary supplementation of AC may represent a minimally invasive approach to mitigate health risks associated with PFAS exposure. Importantly, access to an effective pharmacological method for lowering circulating PFAS levels is critical not only for communities subjected to significant contamination but also for the general population experiencing routine background exposure from everyday products containing PFAS.[29] Further research is warranted to address the possible role of AC treatment in reducing the blood levels of PFAS.

■ ASSOCIATED CONTENT

Supporting Information

The Supporting Information is available free of charge at https://pubs.acs.org/doi/10.1021/acs.chemrestox.5c00510.

Supplemental Table S1: Working concentrations of PFAS solutions; Supplemental Table S2: Recipe for PFAS calibration curve standards solutions; Supplemental Table S3: Parameters of LC-MS/MS analysis of PFAS; Supplemental Table S4: Molecular descriptors of tested PFAS; Supplemental Figure S1: 0−48 h analysis of PFOA removal from simulated bile juice by activated charcoal; Supplemental Figure S2: Row isothermal adsorption curves of PFAS on activated charcoal; Supplemental Figure S3: Fitting analysis curves of isothermal adsorption of PFAS on activated charcoal (PDF)

■ AUTHOR INFORMATION

Corresponding Author

ntonio Marcomini − *DAIS-Department of Environmental Sciences, Informatics and Statistics, University Ca Foscari of Venezia, Venezia 30172, Italy*; Email: marcomini@unive.it

Authors

lessandro Bonetto − *DAIS-Department of Environmental Sciences, Informatics and Statistics, University Ca Foscari of Venezia, Venezia 30172, Italy*

Luca De Toni − *Department of Medicine, Unit of Andrology and Reproductive Medicine, University of Padova, Padova 35128, Italy*; orcid.org/0000-0003-4958-5217

ndrea Di Nisio − *Department of Psychology and Health Sciences, Pegaso University, Napoli 80143, Italy*

Laura Pagnin − *DAIS-Department of Environmental Sciences, Informatics and Statistics, University Ca Foscari of Venezia, Venezia 30172, Italy*

lberto Ferlin − *Department of Medicine, Unit of Andrology and Reproductive Medicine, University of Padova, Padova 35128, Italy*

Carlo Foresta − *Department of Medicine, Unit of Andrology and Reproductive Medicine, University of Padova, Padova 35128, Italy*

Complete contact information is available at: https://pubs.acs.org/10.1021/acs.chemrestox.5c00510

Author Contributions

§A.B. and L.D.T. share equal contribution.

Author Contributions

Conceptualization: A.D.N., L.D.T., and C.F. **Data curation:** A.B., L.D.T., and A.M. **Formal analysis:** A.D.N. and L.D.T. **Funding acquisition:** C.F. **Investigation:** A.B. and L.P. **Methodology:** A.B. and A.M. **Project administration:** C.F. and A.F.. **Resources:** C.F. and A.F. **Software:** A.B. and L.P. **Supervision:** C.F., A.F., and A.M. **Validation:** A.B. **Visualization:** A.D.N., L.D.T., and A.M. **Writing − original draft:** A.B., A.D.N., and L.D.T. **Writing − review and editing**: C.F. and A.M.

Funding

The study was funded by the Local Health Authority ULSS 8 BERICA, with a release dated May 3, 2024, protocol no. 47889, and the Local Health Authority ULSS 9 SCALIGERA, with a release dated August 16, 2024, protocol no. 137183, upon recommendation of the Veneto Region dated July 31, 2024, protocol no. 385739, as part of the project ″Proposal for an experimental study for the reduction of perfluoroalkyl substances (PFAS) in exposed subjects through treatment with vegetable activated carbon.″

Notes

The authors declare no competing financial interest.

■ REFERENCES

(1) Harada, K.; Inoue, K.; Morikawa, A.; Yoshinaga, T.; Saito, N.; Koizumi, A. Renal Clearance of Perfluorooctane Sulfonate and Perfluorooctanoate in Humans and Their Species-Specific Excretion. *Environ. Res.* **2005**, *99* (2), 253−261.

(2) Fromme, H.; Mosch, C.; Morovitz, M.; Alba-Alejandre, I.; Boehmer, S.; Kiranoglu, M.; Faber, F.; Hannibal, I.; Genzel-Boroviczény, O.; Koletzko, B.; Völkel, W. Pre- and Postnatal Exposure to Perfluorinated Compounds (PFCs). *Environ. Sci. Technol.* **2010**, *44* (18), 7123−7129.

(3) Thomsen, C.; Haug, L. S.; Stigum, H.; Frøshaug, M.; Broadwell, S. L.; Becher, G. Changes in Concentrations of Perfluorinated Compounds, Polybrominated Diphenyl Ethers, and Polychlorinated Biphenyls in Norwegian Breast-Milk during Twelve Months of Lactation. *Environ. Sci. Technol.* **2010**, *44* (24), 9550−9556.

(4) Olsen, G. W.; Burris, J. M.; Ehresman, D. J.; Froehlich, J. W.; Seacat, A. M.; Butenhoff, J. L.; Zobel, L. R. Half-Life of Serum Elimination of Perfluorooctanesulfonate,Perfluorohexanesulfonate, and Perfluorooctanoate in Retired Fluorochemical Production Workers. *Environ. Health Perspect.* **2007**, *115* (9), 1298−1305.

(5) Perez, F.; Llorca, M.; Farré, M.; Barceló, D. Automated Analysis of Perfluorinated Compounds in Human Hair and Urine Samples by Turbulent Flow Chromatography Coupled to Tandem Mass Spectrometry. *Anal. Bioanal. Chem.* **2012**, *402* (7), 2369−2378.

(6) Zhang, Y.; Beesoon, S.; Zhu, L.; Martin, J. W. Biomonitoring of Perfluoroalkyl Acids in Human Urine and Estimates of Biological Half-Life. *Environ. Sci. Technol.* **2013**, *47* (18), 10619−10627.

(7) Cao, H.; Zhou, Z.; Hu, Z.; Wei, C.; Li, J.; Wang, L.; Liu, G.; Zhang, J.; Wang, Y.; Wang, T.; Liang, Y. Effect of Enterohepatic Circulation on the Accumulation of Per- and Polyfluoroalkyl Substances: Evidence from Experimental and Computational Studies. *Environ. Sci. Technol.* **2022**, *56* (5), 3214−3224.

(8) Colpo, A.; Astolfi, L.; Tison, T.; De Silvestro, G.; Marson, P. Impact of COVID-19 Pandemic in the Activity of a Therapeutic Apheresis Unit in Italy. *Transfusion and Apheresis Science* **2020**, *59* (6), No. 102925.

(9) Genuis, S. J.; Curtis, L.; Birkholz, D. Gastrointestinal Elimination of Perfluorinated Compounds Using Cholestyramine and Chlorella Pyrenoidosa. *ISRN Toxicol.* **2013**, *2013*, 1−8.

(10) Andersson, A. G.; Xu, Y.; Kärrman, A.; Cederlund, J.; Lindh, C. H.; Pineda, D.; Fletcher, T.; Jakobsson, K.; Li, Y. Serum, Urinary and Fecal Concentrations of Perfluoroalkyl Substances after Interventions

with Cholestyramine/Colesevelam and Probenecid − Cross-over Trials in Ronneby, Sweden. *Environ. Int.* **2025**, *204*, No. 109794.
(11) Genuis, S. J.; Birkholz, D.; Ralitsch, M.; Thibault, N. Human Detoxification of Perfluorinated Compounds. *Public Health* **2010**, *124* (7), 367−375.
(12) Scaldaferri, F.; Pizzoferrato, M.; Ponziani, F. R.; Gasbarrini, G.; Gasbarrini, A. Use and Indications of Cholestyramine and Bile Acid Sequestrants. *Int. Emerg. Med.* **2013**, *8* (3), 205−210.
(13) Ahrens, L.; Lundgren, S.; McCleaf, P.; Köhler, S. Removal of Perfluoroalkyl Substances (PFAS) from Different Water Types by Techniques Based on Anion Exchange (AIX), Powdered Activated Carbon (PAC), Iron(III) Chloride and Nanofiltration (NF) Membrane − A Systematic Comparison. *Science of The Total Environment* **2025**, *970*, No. 179004.
(14) Xiao, C.; Chen, J.; Rehman, M.; Yang, L.; Tan, S.; Fahad, S.; Deng, G.; Shen, S. Synergistic Enhancement of Yunnanopilia Longistaminea Growth, Quality, and Soil Dynamics Using Biochar and Methyl Jasmonate. *Plant Science* **2025**, *359*, No. 112628.
(15) McCleaf, P.; Englund, S.; Ostlund, A.; Lindegren, K.; Wiberg, K.; Ahrens, L. Removal Efficiency of Multiple Poly- and Perfluoroalkyl Substances (PFASs) in Drinking Water Using Granular Activated Carbon (GAC) and Anion Exchange (AE) Column Tests. *Water Res.* **2017**, *120*, 77−87.
(16) Rahman, S. U.; Han, J.-C.; Yasin, G.; Imtiaz, M. T.; Zhao, X.; Alharbi, S. A.; Alfarraj, S.; Alarfaj, A. A. Synergetic Effects of Potassium and Biochar on Morphological, Physiological, and Biochemical Attributes of Maize Crop Grown under Different Levels of Drought Stress. *BMC Plant Biol.* **2025**, *25* (1), 402.
(17) Giovannetti, S.; Barsotti, G.; Cupisti, A.; Dani, L.; Bandini, S.; Angelini, D.; Antonelli, A.; Salvadori, M.; Urti, D. A. Oral Activated Charcoal in Patients with Uremic Pruritus. *Nephron* **2004**, *70* (2), 193−196.
(18) Buckley, N. A.; Dawson, A. H.; Juurlink, D. N.; Isbister, G. K. Who Gets Antidotes? Choosing the Chosen Few. *Br. J. Clin. Pharmacol.* **2016**, *81* (3), 402−407.
(19) Mozaffari Majd, M.; Kordzadeh-Kermani, V.; Ghalandari, V.; Askari, A.; Sillanpää, M. Adsorption Isotherm Models: A Comprehensive and Systematic Review (2010−2020). *Science of The Total Environment* **2022**, *812*, No. 151334.
(20) EFSA Panel on Dietetic Products, Nutrition and Allergies (NDA). Scientific Opinion on the Substantiation of Health Claims Related to Activated Charcoal and Reduction of Excessive Intestinal Gas Accumulation (ID 1938) and Reduction of Bloating (ID 1938) Pursuant to Article 13(1) of Regulation (EC) No 1924/2006. *EFSA J.* **2011**, *9* (4), 2049.
(21) Abulikemu, G.; Pressman, J. G.; Sorial, G. A.; Sanan, T. T.; Haupert, L. M.; Burkhardt, J. B.; Smith, S. J.; Kleiner, E. J.; Stebel, E. K.; Gray, B. N.; Gastaldo, C. X.; Hughes, E. W.; Pedigo, S. G.; Wahman, D. G. Perfluoroalkyl Chemical Adsorption by Granular Activated Carbon: Assessment of Particle Size Impact on Equilibrium Parameters and Associated Rapid Small-Scale Column Test Scaling Assumptions. *Water Res.* **2025**, *271*, No. 122977.
(22) Teng, B.; Zhao, Z.; Wu, J.; Xia, L.; Wang, Y.; Wang, H.; Yemele, O. M.; Adnan, M. Study on the Effect of Alginate Coated Ca-Fe Bimetallic Composite Biochar Microspheres on the Removal of Short-Chain PFAS. *Environ. Res.* **2025**, *285*, No. 122395.
(23) Sanjel, B.; Shim, W.-S. Recent Advances in Understanding the Molecular Mechanisms of Cholestatic Pruritus: A Review. *Biochimica et Biophysica Acta (BBA) - Molecular Basis of Disease* **2020**, *1866* (12), No. 165958.
(24) Quattrini, S.; Pampaloni, B.; Brandi, M. L. Natural Mineral Waters: Chemical Characteristics and Health Effects. *Clin. Cases Min. Bone Metab.* **2016**, *13*, 173.
(25) Cao, J.; Feng, S.; Dolatabad, A. A.; Zhi, Y.; Deng, B.; Liu, C.; Lyu, X.; Christensen, C. S. Q.; Pignatello, J. J.; Ni, P.; Lin, S.; Wei, Z.; Xiao, F. PFAS Removal from Reverse Osmosis and Nanofiltration Brine by Granular Activated Carbon: Thermodynamic Insights into Salinity Effects. *Water Res.* **2025**, *282*, No. 123758.
(26) Militao, I. M.; Roddick, F.; Fan, L.; Zepeda, L. C.; Parthasarathy, R.; Bergamasco, R. PFAS Removal from Water by Adsorption with Alginate-Encapsulated Plant Albumin and Rice Straw-Derived Biochar. *Journal of Water Process Engineering* **2023**, *53*, No. 103616.
(27) Largitte, L.; Pasquier, R. A Review of the Kinetics Adsorption Models and Their Application to the Adsorption of Lead by an Activated Carbon. *Chem. Eng. Res. Des.* **2016**, *109*, 495−504.
(28) Ogata, Y.; Imaoka, A.; Akiyoshi, T.; Ohtani, H. Effects of Food Type on the Extent of Drug-Drug Interactions between Activated Charcoal and Phenobarbital in Rats. *Drug Metab. Pharmacokinet.* **2019**, *34* (4), 287−291.
(29) Buekers, J.; Colles, A.; Cornelis, C.; Morrens, B.; Govarts, E.; Schoeters, G. Socio-Economic Status and Health: Evaluation of Human Biomonitored Chemical Exposure to Per- and Polyfluorinated Substances across Status. *Int. J. Environ. Res. Public Health* **2018**, *15* (12), 2818.

https://doi.org/10.1021/acs.chemrestox.5c00510
Chem Res Toxicol 2026 39 900−907